Seismicity related to the hydraulic stimulation of GRT1, Rittershoffen, Alsace, France

Olivier Lengliné[1], Mohamed Boubacar[1], Jean Schmittbuhl[1].

[1] EOST-IPGS, Université de Strasbourg/CNRS, 5 rue René Descartes, 67084 Strasbourg, France

lengline@unistra.fr

Keywords: Induced Seismicity, Template-Matching.

ABSTRACT

The ECOGI joint-venture is developing a deep geothermal project at Rittershoffen, 6 km east of Soultz-sous-Forêts, in Northern Alsace. For this purpose, at the end of 2012, a first well (GRT1) was drilled to 2580 m depth through Triassic-sediments and into the crystalline basement. In order to enhance the reservoir permeability, a hydraulic stimulation was performed in the GRT1 well in June 2013. The hydraulic stimulation in GRT1 lasted 2 days (27 and 28 June 2013) and was recorded by a dedicated seismic network. The seismic activity related to the GRT1 hydraulic stimulation was processed in real-time and gave rise to a first seismicity catalogue composed of a total of 212 events, from the 27 of June to the 4th of July 2013. The catalogue reveals that the seismicity stopped shortly after injection, but started again after 4 completely quiet days on July 2nd, in the form of an intense seismic swarm that lasted less than one day. In order to understand how this second crisis developed several days after the injection stopped we apply a dedicated set of tools to recover and locate the most precisely as possible the earthquakes that occurred during this sequence. We are able to detect and locate precisely 1156 events. We show that these events that occurred during the injection define a planar structure where we observe migration of the seismicity. Based on our precise relocations we can also identify that the events of the second crisis occurred on a different structure probably activated by slow aseismic movements.

1. INTRODUCTION

Understanding how the injection of fluids in the crust is linked to the occurrence of earthquakes is of primary importance for the development of geothermal energy. Tracking and understanding this seismicity is important as it both poses a risk to the nearby population and to the infrastructures but also provides information about the reservoir mechanics and the fluid pathway. However modelling the direct impact of the fluid injection on the induced events is not straightforward as it involves the couplings of various processes. Indeed the nucleation of earthquakes is affected both by the existing fractures and faults within the reservoir, the mechanical and chemical impact of the fluid flow, and the temperature variations which all interacts with each other. Most of these parameters are usually not known precisely neither monitored continuously at depth during the injection such that it is difficult to observe their influence on the development of the earthquake activity.

The clear identification of the role of each of these parameters on the seismicity is also restricted by the limited resolution that can be achieved on the earthquake detection and locations. Indeed, the structures activated by fluid injection are usually of very small scale compared to the uncertainties associated with the earthquake locations. It thus requires a dedicated seismological network and processing in order to record and locate precisely the associated seismic activity and highlight the orientation of the active structures.

Here we analyze the earthquake activity that develops during the hydraulic injection in the well GRT1 in Rittershoffen, France. This well is part of a deep geothermal project at Rittershoffen, 6 km east of Soultz-sous-Forêts, in Northern Alsace developed by the ECOGI joint-venture. For this purpose, at the end of 2012, a first well (GRT1) was drilled to 2580 m depth through Triassic-sediments and into the crystalline basement. In order to enhance the reservoir permeability, a hydraulic stimulation was performed in the GRT1 well in June 2013. The hydraulic stimulation in GRT1 lasted 2 days (27 and 28 June 2013) and was recorded by a dedicated seismic network (*Maurer et al.,* (2015), *Baujard et al.,* (2016)). The seismic activity related to the GRT1 hydraulic stimulation was processed in real-time and gave rise to a first seismicity catalogue composed of a total of 212 events, from the 27 of June to the 4th of July 2013 (*Maurer* et al., 2015). The catalogue reveals that the seismicity stopped shortly after injection, but started again after 4 completely quiet days on July 2nd, in the form of an intense seismic swarm that lasted less than one day. We see that given the current state of stress of the area, the strength of the rock mass forming the reservoir and the orientation of the main activated structures, we can propose a logical

geomechanical model for the development of the observed seismicity.

2. DATA

The seismic network around the Rittershoffen geothermal field at the time of the injection of June 2013 was composed of 18 surface stations in total. The recording sampling frequency of these stations is distributed as follows: 9 at 150 HZ, 4 at 100 Hz and 5 at 300 Hz.

A first detection was performed from the recorded continuous signal at all these stations. We use a Short Term Average / Long Term Average (STA/LTA) approach (*Earle & Shearer, 1994*) to detect possible seismic events. All the seismic signals were first filtered between 10 and 40 Hz, the STA is computed over 1s and the LTA over 5s of signal. We set a detection when at least 3 stations reach the STA/LTA threshold fixed a 2. This leads to 946 detections. We then reviewed manually all detections to discard false detection and only keep clear seismic events. We then pick visible P and S arrival times for these events. Location of the events based on the picking arrival times is then obtained by the software HYPOCENTER using a 1D velocity model of the area. It finally results in a set of 674 seismic events that could be located with this approach.

3. DETECTIONS

In order to improve the seismic catalogue we are interested in recovering possible events that were missed during the previous procedure. There are several reasons that explain why an event gets undetected during the STA/LTA procedure. This could be because of a low signal to noise ratio at a sufficient number of stations or events occurring too close in time. It is also possible that some events were detected by the STA/LTA procedure but could not be located confidently because of too few or inconsistent picks resulting in the removal of these events during latter processing stages. All these factors can result in numerous missed events. This is particularly true for the seismicity we are investigating that occurred in a densely populated area with numerous noise sources masking the earthquake signal (*Lehujeur et al., 2015*). The template matching approach use a known seismic signal in order to detect newer events similar to the tested one. This technique has the ability to detect events even when the signal to noise ratio at an individual station is lower than 1. It however requires the knowledge of some template events to which we will compare the continuous seismic signal. The choice of these events will affect the final set of newly detected events, as we will detect mainly similar events to the tested ones. It implies that the newly detected events are necessarily not located too far from the template event because otherwise waveforms will not be similar and stacking the correlation signals at different stations after correcting from travel times will not result in a coherent stack.

One could consider all the detected events as possible templates events. This approach will be quite unnecessarily time consuming as many detected events are similar such that it will be like processing several times the same data and producing the same results. Furthermore, because some identified events have a low signal to noise ratio, it is possible that at some stations the correlation detector will mainly correlate with the noise source and not the earthquake signal. In this case it will produce multiple false detections.

To overcome these difficulties, we consider here a different approach. We first group all located events into clusters of similar waveforms. We compute the correlation matrix between all events around the P-wave on 128 samples long window filtered between 8 and 25 Hz. If the mean correlation coefficient at least at 3 stations is higher than 0.8, we associate the two events into the same cluster. We finally keep the 13 clusters with at least 2 events. For each group we stack the waveforms of all events in the group in order to create a synthetic waveform representing the average waveform of the events of the group. Events are first aligned on the P-wave arrival before the stacking is performed at all possible stations. We thus create synthetic template signals for the 13 groups of events. This approach is somewhat similar to the subspace detector but here we consider only the first vector of the singular value decomposition that represents the stack of the events (*Harris, 2006; Barrett and Beroza, 2014*).

The template matching approach is performed by running the template signal at 3 stations and computing the correlation coefficient at each time step. The three selected stations (KUHL, BETS, RITT) are the three closest stations from the injection point; they are distributed with a good azimuthal coverage relative to the injection point. After the correlation coefficient is obtained at an individual station for a given template event we correct from the travel time delays between stations. This restricts the detections of new events to occur in proximity of the template event. In order to relax this criterion we allow for a 0.5 s spread of the correlation coefficient before stacking the correlation signal at the different stations. It thus allows the possible detection with a somewhat similar waveform to the template but not located exactly in the same area.

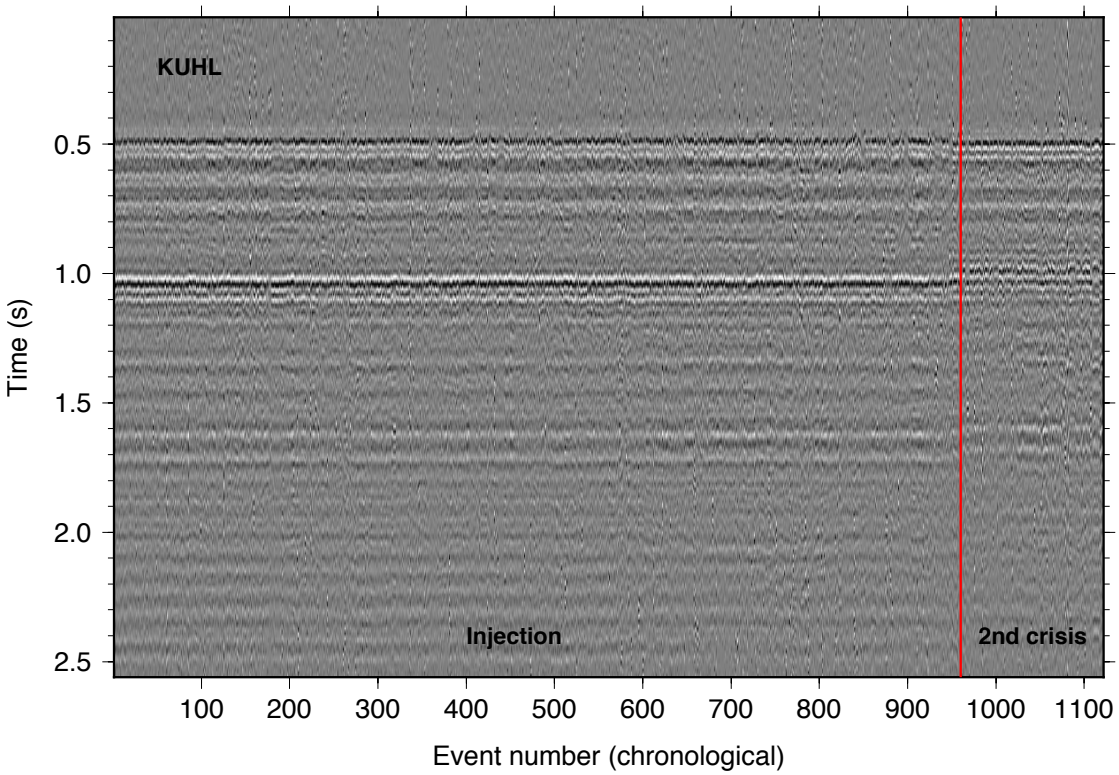

Figure 1: Recorded signals on the vertical component at station KUHL around the P-wave arrival of the 1156 relocated events. Each trace is normalized by its maximum amplitude. We can notice the P-wave arrival around 0.5s and S-wave arrival around 1.0s. We observe the very high similarity between all events during the injection period and during the second crisis.

We consider all parts of the correlation signal with a correlation coefficient higher than 40% as a possible detection. If multiple templates detect the same event we only consider one detection associated with the template for which the correlation coefficient is the highest. This leaves us with 1395 events from the original set of 13. For all these new detections we extract the seismic waveform on all stations around the P-wave arrival (e.g. Figure **1**).

4. RELOCATIONS

We compute travel time delays between all the 1156 detected events. Delays are computed on 128 samples long windows filtered between 8 and 25 Hz and centred on the P-wave arrival. Travel time delays associated with a correlation coefficient higher than 0.5 are then used for relocation. The relocation is performed from the Software HYPODD (*Waldhauser and Ellsworth, 2000*) where we set the initial position of all the events to be located at the injection point.

A total of 1124 events can be relocated from the initial set of events. In order to analyse only well located events we further restrict our analysis to the events that are linked to other events by at least 150 differential travel times data.

Relocations highlight a streak of earthquake located close to the injection point with an azimuth of around N20°E (Figure **2**). All the events of this streak are located in a depth range of around 400m around the injection depth. These events correspond to the first crisis that occurred during the injections. We observe that events in this streak are migrating slowly towards the SW (Figure **3**). Another cluster of earthquakes occurred during the second crisis and is located to the NE of the injection point. There is a clear spatial separation between these two clusters.

5. DISCUSSION

The state of stress in the investigated area has been extensively discussed in a number of studies mainly from measurements performed in the wells of the Soultz-sous-Forêts geothermal site. As this geothermal zone is located less than 10 km away from the current site and as no major structural element is located between these two sites, we will assume that they both are influenced by the same regional stress field, i.e. as proposed in *Cornet et al.*, 2007

$$S_H = S_v \quad [1]$$

$$S_h = 0.54\, S_v \quad [2]$$

$$S_v = 33.8 + 0.0255(z\text{-}1377) \quad [3]$$

with S_H the maximum horizontal stress, S_h, the minimum horizontal stress and S_v the vertical stress. The depth z is in meters and the stresses are in Pa. The direction of S_H has been found to vary with depth. Here we are dealing with a limited vertically extended structure that does not go beyond 2400m depth. We

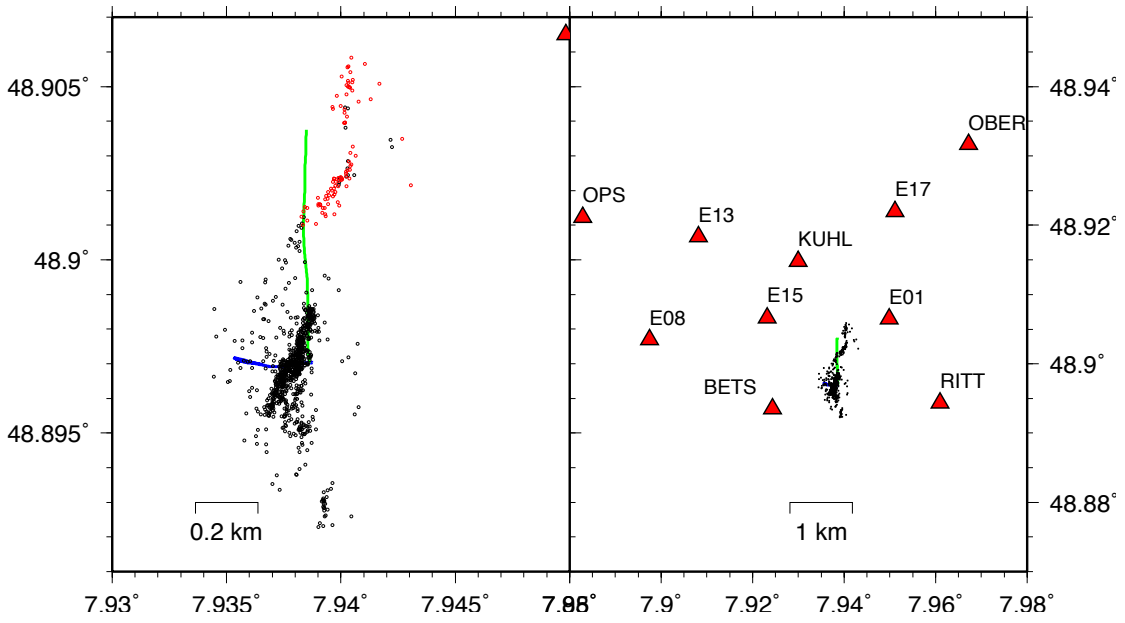

Figure 2: Left: Relocations of events that occurred during the injection (black) and during the second crisis (red). The blue and green lines are the surface projection of the two boreholes, GRT1 and GRT2 respectively. Right: Same as figure on the left but seen at farter distance. The red triangles refer to seismic stations labelled with their names

can then consider that the orientation of S_H is constant with an azimuth of N170°E.

Under such a regional stress field and considering an internal friction coefficient of μ_i=0.9 with a cohesion C_0=1 MPa, as proposed by *Cornet et al*., 2007 for the strong patches on the activated structure, makes the nucleation sites for earthquakes, 2-3 MPa away from failure initially. Fluid injection will cause a reduction in the effective normal stress and bring closer to failure the seismic patches on the fault plane. Interestingly we notice that the earthquake activity does not start immediately at the time of the injection but only at 11:00 UTC when the flow rate was increased from 27l/s to 40l/s. At this stage the downhole pressure gauge reaches 2.5 MPa. This value is in agreement with the value predicted by the Coulomb failure theory. At this point the most favourable plane for failure is a plane oriented 23 degrees from the direction of S_H. Seismicity outlines thus a plane that is almost already favourably oriented and which needs only an extra fraction of stress compared to rupture. The fault plane where seismicity occurs is also visible form borehole imaging as the most permeable structure encountered during the logging. Indeed, it is observe from acoustic image a wide fracture with an approximate azimuth N-S and with a 70° dip towards the west (*Vidal* et al., 2016).

It is difficult to explain the occurrence of the earthquakes of the second crisis only from the diffusion of the injected fluid. Indeed, in this case we would rather expect a continuous seismic activity over the entire period extending from the shut-in to this second crisis. Such a prolonged activity after the end of injection is very often encountered in geothermal exploitation. Furthermore, as the over-pressure in the well reaches almost 0 MPa at the end of the 28th June it is difficult to propagate such a pressure front with no over-pressure at the source. These observations points out to another process as being responsible of the observed activity. We suppose that aseismic slip took place on the imaged fault during the first crisis. The slip on this fault plane produce a stress change of nearly 5 bars to the structure located to the north and brings this structure closer to failure. It is then likely that this increased Coulomb stress cause the earthquake activity that occurs 4 days after. This could be notably explained by the non-linear nucleation of the slip instability in the rate-and-state friction model and the clock advance related to such stress changes (*Dieterich*, 1994 *Gomberg* et al., 1998).

6. CONCLUSION

The earthquakes associated with the first crisis, during the injection, present the features of fluid induced seismicity. They are located at short distance from the injection point and show a migration from this point. We however notice at the end of the injection that several events occur on a different structure to the north. The second crisis, which occurred after 4 quiet days, is located on a different sub-parallel structure compared to the first one. All events occurred in a very short time period during this crisis. It suggests that the events associated with this crisis have a different triggering origin than the injection-induced events and are probably triggered by stress changes induced by slow aseismic movements on the main structure.

REFERENCES

Barrett, S. A., & Beroza, G. C. (2014). An empirical approach to subspace detection. *Seismological Research Letters*, *85*(3), 594-600.

Cornet, F. H., Bérard, T., & Bourouis, S. (2007). How close to failure is a granite rock mass at a 5km depth?. *International Journal of Rock Mechanics and Mining Sciences*, *44*(1), 47-66.

Dieterich, J. (1994). A constitutive law for rate of earthquake production and its application to earthquake clustering. *Journal of Geophysical Research, 99*(B2), 2601-2618.

Earle, P. S., & Shearer, P. M. (1994). Characterization of global seismograms using an automatic-picking algorithm. *Bulletin of the Seismological Society of America*, *84*(2), 366-376.

Gomberg, J., Beeler, N. M., Blanpied, M. L., & Bodin, P. (1998). Earthquake triggering by transient and static deformations. *Journal of Geophysical Research*, *103*(B10), 24411-24426.

Harris, D. B. (2006). *Subspace detectors: theory*. United States. Department of Energy.

Lehujeur, M., Vergne, J., Schmittbuhl, J., & Maggi, A. (2015). Characterization of ambient seismic noise near a deep geothermal reservoir and implications for interferometric methods: a case study in northern Alsace, France. *Geothermal Energy*, *3*(1), 1-17.

Vidal, J., Genter, A. & Schmittbuhl, J. (2016), Pre- and post-stimulation characterization of geothermal well GRT-1, Rittershoffen, France: insights from acoustic image logs of hard fractured rock. *Geophys. J. Int.,* in press

Waldhauser, F., & Ellsworth, W. L. (2000). A double-difference earthquake location algorithm: Method and application to the northern Hayward fault, California. *Bulletin of the Seismological Society of America*, *90*(6), 1353-1368.

Acknowledgements

This study is supported by the LABEX G-EAU-TEHERMIE profonde.